Available online at www.sciencedirect.com

ScienceDirect

Procedia Structural Integrity 68 (2025) 534–539

Structural Integrity Procedia

www.elsevier.com/locate/procedia

European Conference on Fracture 2024

# Influence of vanadium on microstructure and mechanical properties of high-alloyed steel

Aleksandar Todić[a], Milan T. Djordjević[a], Dušan Arsić[b,*], Ružica R. Nikolić[c], Djordje Ivković[b], Dragan Cvetković[d]

[1]*Faculty of Technical Sciences, University of Priština, Knjaza Miloša 7, 38220, Kosovska Mitrovica, Serbia*
[2]*Faculty of Engineering, University of Kragujevac, Sestre Janjić 6, 34000, Kragujevac, Serbia*
[3]*Research Centre, University of Žilina, Univerzitna 8215/1, 010 01 Žilina, Slovakia*
[4]*Institute for Information Technologies, University of Kragujevac, Jovana Cvijića bb, 34000 Kragujevac, Serbia*

**Abstract**

In addition to new, modern non-metallic materials that successfully replace metallic materials in certain fields, steel materials are still widely used in technical practice. This trend will continue for many years. For this reason, there is a need to develop new types of steel with better properties alongside existing ones. The group of newer steels with relatively high values of hardness and toughness includes Cr-Mo steels with high vanadium content. For the investigations in this study, the steel X180CrMo12-1 was used, with varying vanadium content ranging from 0.5% to 3%. Modern equipment was used for the conducted research, including chemical composition analysis, observation of the shape of metallic grains and carbide networks, friction and wear resistance testing, as well as electrochemical characterization. The aim of the conducted research is to determine the composition of carbides, microstructure, morphology, and to evaluate their impact on material characteristics. Steel samples were experimentally tested using scanning electron microscopy with energy-dispersive spectrometry (SEM-EDS) and X-ray diffraction analysis (XRD).

© 2025 The Authors. Published by ELSEVIER B.V.
This is an open access article under the CC BY-NC-ND license (https://creativecommons.org/licenses/by-nc-nd/4.0)
Peer-review under responsibility of ECF24 organizers

*Keywords:* Chemical composition, vanadium, carbides, microstructure, mechanical properties

* Corresponding author. Tel.: +381642769381
*E-mail address:* dusan.arsic@fink.rs

2452-3216 © 2025 The Authors. Published by ELSEVIER B.V.
This is an open access article under the CC BY-NC-ND license (https://creativecommons.org/licenses/by-nc-nd/4.0)
Peer-review under responsibility of ECF24 organizers
10.1016/j.prostr.2025.06.093

## 1. Introduction

To achieve optimal mechanical characteristics of a particular type of steel, various elements are alloyed into the metal. During crystallization, these chemical elements form compounds—carbides—at the grain boundaries and within the metallic matrix, Lin, Y., et al. (2010). Similar materials can also be used to hard weld parts exposed to intense wear for operation in non-lubricated conditions, Arsić, D., et al. (2016).
The tested material is steel X180CrMo12-1, which contains 1.8% carbon, 12% chromium, 1% molybdenum, 0.5% manganese, and a variable vanadium content ranging from 0.5% to 3% (Tab. 1). This steel belongs to the group of quenchable steels, Todić, A. et al. (2011). The objective of the research is to determine the chemical composition of the carbides and to investigate the influence of vanadium and its carbides on changes in the microstructure, wear resistance, and friction resistance of the tested material, Hu, J., et al. (2016), Tlili, B., et al. (2016), Todić, A., et al. (2022), Harouz, R., et al. (2022).

## 2. Experiment plan

The samples for metallographic examinations were prepared using standard procedures, cast by the $CO_2$ casting method in sand molds. Melting was performed in a medium-frequency induction furnace, ASEA Brown Boveri – ABB, type ITMK-500, Todić, A., et al. (2012). The samples measured 10×10×10 mm, intended for electron microscopy with a planned chemical composition. The samples contained 0.5% V and other alloying elements as specified in Table 1.

Table 1. Chemical composition of the sample

| C | Cr | Mo | S | Si | P | Mn | Al | Ni | V |
|---|---|---|---|---|---|---|---|---|---|
| 1.753 | 11.754 | 1.125 | 0.035 | 0.514 | 0.034 | 0.533 | 0.02 | 0.16 | 0.502 |

After casting, the samples were improved (quenched and tempered) at a temperature of 250°C. Post heat treatment, slight deviations in geometric shape and dimensional changes were observed in the samples. Therefore, mechanical processing was applied using lubricants and cooling agents at room temperature. The mechanical processing was performed on a surface grinding machine. Grinding removed irregularities and impurities, with constant heat removal. The defective layer was removed with minimal cutting depth in multiple passes, down to the desired dimensions of 10×10 mm. Given the small machining allowances, the total grinding depth did not exceed 0.5 mm, thus preventing any potential change in surface structure.

For determining the chemical composition and microstructure, electron microscopy (SEM-EDS) was used. The scanning electron microscope used was a JEOL model JSM-6610LV. SEM-EDS was utilized to determine the chemical composition at specific points of the phases present on the sample surface. Additionally, a mapping of the influential chemical elements was performed to understand and detect the phases present on the tested sample.

Further investigations were conducted using X-ray diffractometry. Identification and calculation of lattice parameters were performed. This analysis was carried out on a D8 ADVANCE device from Bruker. The device is equipped with a dynamic scintillation detector and a ceramic X-ray Cu tube (KFL-Cu-2K) with a scanning angle range from 10 to 150°. Samples for this analysis were ground and converted into fine powder. Working parameters included a step size of 0.02 and a step time of 20 seconds. Detection was conducted using the Topas 4.2 software package with data from the ICCD database PDF-2 Release 2013.

For testing the wear resistance of the aforementioned steel, a CSM Nanotribometer, "Ball-on-plate" linear-reciprocating type, was used. The ball material used for the friction and wear process was hard metal with a diameter of 1.5 mm. The testing conditions were as follows: normal load 1N, sliding speed 10 mm/s, amplitude 0.5 mm, 5000 cycles/10 m, without lubrication. Wear and friction testing was conducted on 4 series of samples with different vanadium percentages. Each sample was tested 5 times, documented with comparative diagrams of friction coefficients and ball penetration depth over time, cycle count, and sliding path. Additionally, photographs of the wear traces on the material and the ball were provided. For analyzing the surfaces of prepared samples and the wear traces, computer-aided optical microscopes from "MEIJI Techno" were used, each equipped with its own illuminator and high-resolution camera.

Hardness testing was conducted following the standard Vickers method procedure. Microhardness was determined using a Digital Microhardness Tester, model DHV-1000. The applied load was 0.245 N, with an indentation time of 20 seconds.

## 3. Results and discussion

Around the martensitic grains, a clearly defined carbide network is observed, with a small portion of carbides finely dispersed within the metal matrix (Fig. 1). The primary type of carbide is $M_7C_3$, and its composition was determined by EDS analysis.

The presence of vanadium, even in small amounts, has a positive effect on high-alloyed Cr-Mo steels. During solidification from the melt, $V_6C_5$ carbide crystals form, which block the further growth of primary austenite dendrites, thereby promoting a fine-grained structure. Vanadium, being a strongly carbide-forming element, not only forms $V_6C_5$ carbide grains but also influences the morphology of $M_7C_3$ carbides. Additionally, it reduces the stability of austenite and generally refines the structure of the metal matrix. Similar to iron, vanadium replaces chromium in the $M_7C_3$ carbide lattice, leading to an increased chromium content in the metal matrix and a higher degree of austenite hardenability.

### *3.1. Microstructure analysis*

In Figure 1, the microstructure of sample I with 1.8% C and 0.5% V is depicted. The figure shows martensitic crystals and a carbide network around the grains of the metal matrix. The eutectic carbide M7C3 forms this network in the alloy structure. It precipitates in the form of lamellae, plates, and rosettes. It can be observed that M7C3 carbide appears in a two-dimensional space as strips. A larger number of these strips are often grouped into bundles with the same spatial orientation, resembling lamellae in two-dimensional space. Points 1 to 5 on the depicted image indicate locations where EDS analysis was performed. Three measurements were taken for each point, and Table 2 displays the average values. The maximum experimental deviations are ±2.0%.

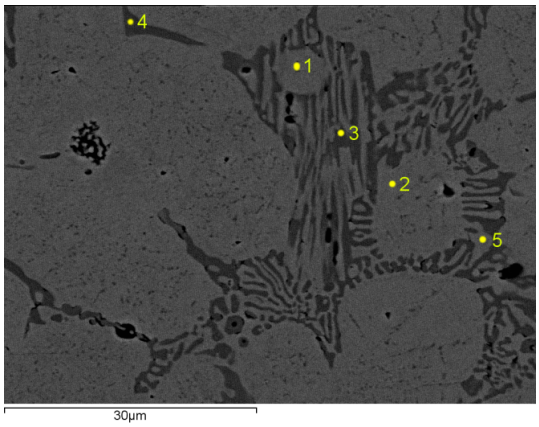


Fig. 1. Microstructure of the sample.

At points 1, 2, and 5, chemical analysis of the metal matrix was conducted, while at points 3 and 4, chemical analysis of the carbide network was performed (Fig. 1). Table 2 shows the chemical analysis of the examined phases in percentages. Figure 2 depicts the microstructure of sample No. II with 1.8% C and 1% V.

The analysis of the metal matrix indicates that it is predominantly martensite with residual austenite, but the increased content of carbon and vanadium suggests the presence of finely dispersed vanadium carbides in the metal matrix.

In addition to SEM-EDS analysis, samples were also examined using XRD analysis. X-ray diffractometry was conducted to determine the phases present in the examined samples.

Table 2. Chemical composition of the sample (tested)

| Measurement points | Element content, % | | | | | | |
|---|---|---|---|---|---|---|---|
| | C | Si | V | Cr | Fe | Ni | Mo |
| 1 | 9.16 | 0.53 | 1.85 | 12.48 | 74.08 | 0.43 | 1.48 |
| 2 | 3.17 | 0.59 | 1.97 | 11.95 | 81.70 | - | 0.6 |
| 3 | 14.54 | - | 9.21 | 32.91 | 41.15 | - | 2.19 |
| 4 | 15.20 | - | 12.76 | 39.67 | 29.33 | - | 3.04 |
| 5 | 8.76 | 0.50 | 1.680 | 10.53 | 77.49 | - | 1.04 |

### *3.2. Determination of the friction coefficient and wear rate*

The coefficient of friction was determined as the average value over the sliding path, i.e., the time of contact achievement. Table 3 provides an overview of friction coefficient values from five measurements for all samples. Additionally, it shows the average friction coefficient values for each sample, along with the standard deviation values.

Table 3. Friction coefficient of the sample

| Measurement points | Friction coefficient, μ |
|---|---|
| 1 | 0.14 |
| 2 | 0.16 |
| 3 | 0.143 |
| 4 | 0.154 |
| 5 | 0.148 |
| Mean value | 0.149 |
| Standard deviation | 0.0106 |

In experimental wear testing in this case, the roughness of contact surfaces and wear of the testing device's ball are disregarded [7]. Therefore, the hardness of the ball material should be higher than that of the material being tested. Despite meeting this condition, wear of the ball is inevitable when testing hard materials. In this specific case, preliminary tests showed that during testing, wear occurred on balls made of $Al_2O_3$, sapphire, and hard metal. Analysis of wear on these ball materials led to the decision to continue testing with the hard metal ball, as it has the most favorable surface geometry and lowest roughness. Pits were observed on the surfaces of $Al_2O_3$ and sapphire balls due to wear, with diameters up to 10μm. The presence of pits on the ball allows accumulation of wear debris and the formation of adherents on the ball's surface. Testing with the hard metal ball showed no presence of adherents on its surface. Adherents on the ball's surface affect both the coefficient of friction and wear values. In tables 4 and 5 are given the measured values of surface areas and lengths of obtained wear tracks and wear rate of the sample.

Table 4. Measured values of surface areas and lengths of obtained wear tracks.

| Measurement points | Friction coefficient, μ | |
|---|---|---|
| | Surface | Length |
| 1 | 59470.27 | 627.45 |
| 2 | 61611.93 | 649.07 |
| 3 | 62021.62 | 683.75 |
| 4 | 57371.95 | 644.74 |
| 5 | 60434.61 | 672.09 |
| Mean value | 60182.08 | - |
| Standard deviation | 1863.844 | - |

Table 5. Wear rate (volume) in $\mu m^3$

| Measurement points | Wear rate (volume) in $\mu m^3$ |
|---|---|
| 1 | 65822.97 |
| 2 | 56690.60 |
| 3 | 57088.88 |
| 4 | 53829.93 |
| 5 | 50842.54 |
| Mean value | 56854.99 |
| Standard deviation | 5608.185 |

On the photographs of wear tracks, the occasional presence of a tribological layer on the contact surface of the tested material is observed (Fig. 2). The formed tribological layer consists of a mixture of the ball material, the tested material, and their oxides. Due to the generation of heat in the thin contact layer, the wear products combine and form a kind of protective layer on the surface of the tested material.

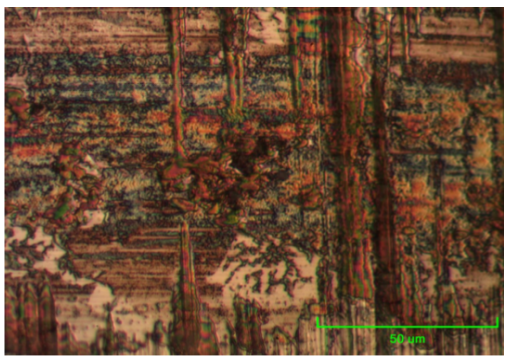


Fig. 2. Enlarged view of the wear track of tested sample

## 4. Conclusion

In this paper, we investigated the influence of vanadium on the hardness, impact toughness, and microstructure of steel containing 1.8% carbon, 12% chromium, and 1.3% molybdenum. With increased vanadium content, the structure

becomes finer, impacting the mechanical properties of the steel, specifically hardness and impact toughness. In the alloy studied, the vanadium content was 0.5% V.

Microstructural examinations confirm that the base of the alloy is martensitic with residual austenite, and a carbide network exists between martensitic crystals. The carbide network consists of $M_7C_3$ crystals with diverse morphologies. Carbides precipitate in the form of lamellae, plates, and rosettes, which are visible in the provided microstructure images. Even with a low vanadium content of 0.5 mass% in the alloy (sample I), noticeable presence of $M_7C_3$ carbides is observed, which appear as rods in two-dimensional space. EDS analysis of the metal matrix confirms the dominance of martensite and residual austenite. The increased carbon content and low percentage of vanadium indicate the presence of finely dispersed vanadium carbides in the metal matrix.

Friction and wear resistance testing indicate that the friction coefficient is stable and does not oscillate across multiple measurement points.

## Acknowledgements

Research presented in this paper was partially financially supported by the project TR35024 of the Ministry of Education, Science and Technological Development of Republic of Serbia.

## References

Lin, Y., Lin, C-C., Tsai, T.H., Lai, H.J., 2010. Microstructure and mechanical properties of 0.63C-12.7Cr martensitic stainless steel during various tempering treatments. Materials and Manufacturing Processes 25(4), 246-248. https://doi.org/10.1080/10426910903426307

Arsić, D., Lazić, V., Mitrović, S., Džunić, D., Aleksandrović, S., Djordjević, M. and Nedeljković, B. 2016. Tribological behavior of four types of filler metals for hard facing under dry conditions, Industrial Lubrication and Tribology, 68(6), 729-736. https://doi.org/10.1108/ILT-10-2015-0156

Todić, A., Čikara, D., Todić, T., Čamagić, I., 2011. The influence of the vanadium content on the toughness and hardness of wear resistant high-alloyed Cr-Mo steel. FME Transactions 39(2), 49-54.

Hu, J., Hu, H., 2016. Friction and wear behavior analysis of the stainless steel surface fabricated by laser texturing underwater. Tribology International 102, 371-377. https://doi.org/10.1016/j.triboint.2016.06.001

Tlili, B., Barkaoui, A., Walock, M., 2016. Tribology and wear resistance of the stainless steel. The sol–gel coating impact on the friction and damage. Tribology International, 102, 348-354. https://doi.org/10.1016/j.triboint.2016.06.004

Todić, A., Djordjević, M. T., Arsić, D., Džunić, D., Lazić, V., Aleksandrović, S., Krstić, B., 2022. Influence of vanadium content on the tribological behaviour of X140CrMo12-1 air-hardening steel. Transactions of FAMENA 46(2), 15-22. https://doi.org/10.21278/TOF.462035021

Harouz, R., Lakehal, A., Khelil, K., Dedry, O., Hashemi, N., Boudebane, S., 2022. Dry sliding friction and wear of the WC/TiC-Co in contact with $Al_2O_3$ for two sliding speeds, FACTA UNIVERSITATIS Series: Mechanical Engineering 20(1), 37-52. https://doi.org/10.22190/FUME200310039H

Todić, A., Čikara, D., Todić, T., Minić, D., Čikara-Anić, D., 2012. Influence of chemical composition on the structure, hardness and toughness of high-alloyed Cr-Mo-V steel. Materials and Manufacturing Processes 27(11), 1193-1197. http://dx.doi.org/10.1080/10426914.2012.663120